Published on *Dyes and Pigments*, 80 (2009) 226-232.

Colour Performance of Ceramic Nano-pigments

P.M.T. Cavalcante[1], M. Dondi[2], G. Guarini[2], M. Raimondo[2], G. Baldi[3]

[1]*Universidade Federal do Rio de Janeiro- PEMM/COPPE, Rio de Janeiro, BR*

[2]*ISTEC-CNR, Institute of Science and Technology for Ceramics, Via Granarolo 64, 48018 Faenza, Italy*

[3]*CERICOL, Centro Ricerche Colorobbia, Via Pietramarina 123, 50053 Sovigliana Vinci, Italy*

Abstract. Ceramic nano-pigments have been recently developed for ink-jet printing decoration of ceramic tiles by the quadrichromy technology (cyan, magenta, yellow, and black colours). The colouring mechanisms and performance of these nano-pigments ($CoAl_2O_4$, Au, $(Ti,Cr,Sb)O_2$, $CoFe_2O_4$) were investigated by DRS, XRD and colourimetry. Nano-pigments were dispersed in several ceramic glazes and glassy coatings and their colour performance compared with that of conventional micro-pigments. Each nano-pigment is characterized by its own colour mechanism and chemico-physical stability in ceramic applications. Intense colours are achievable, besides the very small particle size of pigments (< 50 nm) even though the colour of high quality micro-pigments appears to be more saturated. Limitations to the use of nano-pigments arose for very high firing temperatures (>1200ºC) due to particle growth (e.g. Au) or dissolution in the glassy phase (e.g. titania).

Keywords: ceramic pigments; ceramic tiles; colour; nano-pigments.

1. Introduction

Nano-pigments are organic or inorganic substances, insoluble, chemically and physically inert into the substrate or binders, with a particle size less than 100 nm [1]. Although particles sizes in the 100-200 nm range are required in the current manufacturing practice, nano-pigments have recently gained a wide range of industrial applications [2]. For example, mica-based pigments (particle size ~20 nm) with pearlescent effect are used in cosmetics, automobile coatings, plastics, etc. [3]. In cosmetic applications, both doped TiO_2 and ZnO are being developed for use in sunscreens, in order to avoid the skin damage by sunlight radiation [4]. Novel nano-sized reflecting powders, providing a broad-spectrum protection against UV radiation, are more acceptable from the cosmetic viewpoint because they are flesh-toned and turn invisible when applied [5]. Another application is nano-pigment screen, i.e. a new style phosphor screen applied to cathodic ray tube TVs, exploiting nano-pigment to improve contrast, colour gamut and body colour without additional process or cost [6]. Using smaller pigment particles in the liquid crystal display technology can improve not only the stability of pigment in the dispersion medium, but also colour strength, contrast, and transmittance [7]. Also traditional inorganic pigments, including Titanium Dioxide, Zinc Oxide, Silicon Oxide and Magnesium Oxide, are being available in a nano-size range for use in rubber and plastics, e.g. PE, EVA and PVC [8].

The use of nanoparticles can improve the pigment performance: in the organic coatings, for instance, nano-pigments enhance the tribological and mechanical properties – such as scratch and abrasion resistance, hardness, strain-to-failure – while maintaining toughness [9]. Another effect of nanoparticles, being smaller than the wavelengths of

visible spectrum, is that no scattering and no reflection occur in the visible light range, so the nanocomposite is transparent. This provides the possibility of formulating transparent coatings with good weathering resistance, since fillers can still absorb UV light [9]. Anyway, the greatest problem of using nano-pigments is the fact that the finer the powder the higher the surface area, implying poor mixing and agglomeration phenomena enhanced [1].

The ceramic pigments with particle size in the nanoscale have a massive potential market, because of their high surface area, which assures higher surface coverage, higher number of reflectance points and hence improved scattering. In paint formulations, for example, the small particle size allows uniform dispersion by homogenous mixing with binders, which enhances the mechanical strength of the paint after drying. When properly dispersed, the nanosized pigments exhibit superior effectiveness also in critical abrasive and polishing applications [10].

The literature about ceramic decoration using nanoparticles concerns in most cases pigments promoting a pearlescent or luster aesthetic effect into the glaze. Recent studies of Renaissance and Modern lusters show that these pigments are formed by copper and silver nanocrystals or formed by a thin layer of titanium oxide on a transparent substrate, such as muscovite in the case of pearlescent surfaces [3, 11, 12]. In the luster, separate silver and copper pseudo-spherical nanocrystals appear to be dispersed into the glaze, whose optical properties depend on specific nanostructures of Ag and Cu depositions as well as Cu/Ag ratio, nature of the glaze and, when applied over pre-existing pigments, on the interaction with the underlying material [13].

A novel field of application is ceramic decoration by ink-jet printing, where nano-pigments are able to overcome problems caused by micronized pigments (e.g. nozzles clogging, dispersion instability) [14]. Such problems can be solved by the use of ceramic nano-inks (nanometric particles dispersed in an organic vehicle) which are able to improve the image quality ensuring high reliability to the printing systems [14]. At any rate, the colouring performance of ceramic pigments depends on both optical properties, which are expected to improve in nanoparticles, and chemical stability, since the dissolution rate in glazes is expected to increase with surface area of pigment. The best compromise in conventional ceramic pigments is usually found with particle size distribution in the 1-10 μm range [15]. However, ceramic nano-pigments (10-80 nm) behaved satisfactorily in preliminary printing tests on ceramic tiles, developing intense colours in a wide range of firing temperatures [14].

The aim of this work is to assess both the colouring performance and the potential of nano-pigments in the ceramic tile decoration, especially porcelain stoneware tiles. The rationale consists in nano-pigment application in several ceramic matrices, determination of resulting optical properties and pigment phase composition after firing, including a comparison of colour performance with conventional micro-pigments.

2. Experimental

Four types of nano-pigment suspensions for ink-jet printing in quadrichromy (CMYK: cyan, magenta, yellow and black) were taken into account. These suspensions (nano-inks) were prepared by CERICOL as ceramic oxides or metals synthesized in an organic medium by means of a modified polyol procedure [16]. These pigments were characterized determining (Table 1): particle size distribution by SEM-FEG and STEM (Transmission Electron Microscopy Supra40, Zeiss, Oberkochen, Germany) and by DLS (Dynamic Light Scattering, ZetaSizer-NanoSeries, Malvern Instruments, Malvern, UK);

phase composition by high temperature X-ray powder diffraction (X'Pert Pro, Panalytical, Almelo, The Netherlands) using graphite-monochromated $CuK_{1,2}$ radiation, 10-80 º2Θ range, scan rate 0.02º, 3 s per step).

Each nanoink was applied by dropping 0.05 to 0.1 $mg \cdot cm^{-2}$ on unfired ceramic substrates, controlling penetration depth in order to get the actual pigment concentration. Commercial glassy coatings (F1, F2, F3 and F4), glazes (S1, S2 and S3) and a porcelain stoneware body – each with different chemical and physical properties [17-18] – were selected. These samples were dried and fired in an electric kiln with fast cycle (60 min cold-to-cold) at maximum temperatures ranging from 800 to 1200 ºC. Fired samples were characterized by x-ray diffraction (D500, Siemens, Karlsruhe, Germany; CuK_α radiation, scan rate 0.02 $º2\Theta \cdot s^{-1}$, 5 s per step) in order to determine phase evolution and pigment particle size. This latter was calculated by the Scherrer's equation [19] using FWHM (Full Width at Half Maximum) of the main peaks; instrumental broadening was corrected by measuring the LaB_6 reference material (NIST SRM660a).

The optical absorption spectra of fired samples were recorded in the UV-Visible-NIR range (300-1100 nm) by diffuse reflectance spectroscopy (DRS, λ35, Perkin Elmer, Wellesley, USA) using a $BaSO_4$ integrating sphere and a $BaSO_4$ pellet as white reference. Reflectance (R_∞) was converted to absorbance (K/S) by the Kubelka-Munk equation: $K/S = 2(1- R_\infty) \cdot (2 R_\infty)^{-1}$ [20]. Colourimetric parameters were also evaluated by a portable spectrophotometer (MSXP4000 Hunterlab Miniscan, white glazed tile reference x = 31.5, y = 33.3, illuminant D65, 10º observer) and expressed in the CIELab colour coordinates: L* (100 = white, 0 = black), a* (+ red, - green) and b* (+ yellow, - blue).

In order to compare the colouring performance of nano-pigments with that of conventional ceramic pigments in the tile decoration, four commercial pigments, available as micrometric powder with cyan, magenta, yellow and black colours, were mixed together with the glassy coating F1 and the glaze S1, paying attention to put exactly the same pigment concentration than that applied as nanoinks. Also these samples underwent fast firing and characterization by XRD, UV-Visible-NIR and colourimetric analyses.

3. Results and discussion

3.1. Magenta nano-pigment

Red shades are obtained exploiting the peculiar optical features of metallic gold nanoparticles. In fact, noble metal nanoparticles like gold, silver and copper are strong absorbers and scatterers of visible light, showing a very intense colour. Their unique optical property is due to the collective oscillation of conduction electrons, known as *surface plasmon*, whose resonance causes a strong light absorption in the visible spectrum [21-22]. Energy and shape of the plasmonic band vary depending on size and morphology of gold nanoparticles, which can be estimated on the basis of resonance energy and band width [21-23].

The diffuse reflectance spectra of ceramics coloured with the nanogold pigment exhibit a gaussian-like plasmonic band, characteristic of spherical particles [21-22], quite constant in energy (~19000 cm^{-1} or ~2.3 eV) even in different matrices and firing temperatures (Fig. 1a); it is very similar to that of gold nanoclusters in borosilicate glass [23]. In detail, changes in the band energy and shape can be observed: energy shifts to lower values in glazes, while an increased band width occurs in glassy coating at higher temperatures associated with an increased resonance energy (Fig. 1b).

Resonance energy values are consistent with particle sizes below 20 nm, according to the models in the literature [21-22]. However, wider bands would indicate a particle growth with firing temperatures above 1100 ºC [21,24].

The gold particle size ranges from 40 to 90 nm, as calculated by the Scherrer's equation, in most matrices, although it can reach values around 200 nm in some glazes or glassy coatings (Fig. 2a), particularly F4, that is a borosilicate glass, whose abundant B_2O_3 content (~20%) promotes a fast gold particles growth even at a relatively low firing temperature. Overall, analysing the trend of F1 with firing temperature (Fig. 2b), it can be observed a moderate size growth up to 1100 ºC (20 nm $\rightarrow$ 50 nm) and a considerable coarsening at 1200 ºC (up to 165 nm).

The colourimetric parameters show a deep magenta colour with a red component (a*) ranging from 15 to 33 associated to a poor yellow component (b*) going from 2 to 14 (Table 2). These colour changes mostly depend on the different opacity of ceramic matrices. The magenta colour is very stable in a wide range of temperatures (800-1100ºC), although it turns to be more orange at highest temperature, when an increase of the b* parameter occurs. This is to a large extent due to the broadening of the resonance band, likely connected with the gold particles growth.

The gold nano-pigment is stable into all the ceramic matrices, ensuring an intense magenta colour. Chromatic parameters, and especially the slight colour shift towards the yellow, are mainly affected by the growth of gold particle size, which implies a change in the shape of the plasmonic band as predictable by the literature [21-25] .

Since the magenta nanogold has no equivalent among commercial micro-pigments, two different red colourants were taken into account: cadmium sulfoselenide included into zircon [26] and chromium-doped yttrium aluminium perovskite (YAP) [17,27]. The optical spectra of coloured ceramic wares (Fig. 1c) show the sharp absorption band of Cd(S,Se), cutting all wavelengths from yellow to violet, and the broad bands of nanogold and YAP. The peculiar semiconductor structure of Cd(S,Se) makes its colour performance outstanding as witnessed by very high a* and b* values. The behaviour of gold nano-pigment is close to that of YAP, with a distinctly lower yellow component, making its red coloration purer.

3.2. Cyan nano-pigment

Nano-sized $CoAl_2O_4$ is expected to have a spinel-type structure, with Co^{2+} situated at the tetrahedral site [28] The correspondent microcrystalline pigment is widely used in the ceramic industry as blue colouring agent in glazes and also in the bulk coloration of porcelain stoneware tiles [29-30]. However, in the ink under investigation there is no clue of crystalline phases, as detected by XRD, even after thermal treatment. On the other hand, the optical spectrum of ink is coherent with a hexa-coordinated Co^{2+} ion, being characterized by a broad band centred at 19000 cm^{-1} (Fig. 3a), probably a metallo-organic complex with the glycol medium [31]. It is completely different from the optical spectrum of the commercial $CoAl_2O_4$ micro-pigment, wich exhibits the expected intense bands in the 15000-18000 cm^{-1} range attributable to the $^4A_2$ (^4F) $\rightarrow$ $^2T_1$+^2E (^2G) and $^4T_1$ (^4P) transitions of Co^{2+} in 4-fold coordination [20-31]. Once the ink was applied in the various ceramic matrices, all spectra are similar each other, the main difference being the absorbance, independently on temperature and composition (Fig. 3b and 3c).

Three intense bands are present at ~15000, ~17000 and ~19000 cm^{-1}, which correspond to the electronic transitions of Co^{2+} in tetrahedral coordination in silicate glasses: $^4A_2$ (^4F)$\rightarrow$ $^2T_1$ + ^2E (^2G) $\rightarrow$$^4T_1$ (^4P) and $\rightarrow$ $^2T_2$ (^2G) respectively [32]. The energy of these bands does not vary significantly with temperature, as already known from studies on different silicate glasses [33]. Increased absorbance, observed in glasses and glassy

coating when increasing firing temperature, maybe ascribed to a progressive distortion of the tetrahedral site where the Co^{2+} is accommodated. However, the dissolution of Co^{2+} in the glassy phase is accomplished at temperatures over 900 ºC, as suggested by the fact that the F1 matrix spectrum of the sample fired at 800 ºC is completely different from the others (Fig. 3c). This implies that Co^{2+} is in both 4-fold (band at ~15000 cm^{-1}) and 6-fold coordination (band at ~24000 cm^{-1}).

The colourimetric parameters (Table 2) show excellent blue shades in glazes (-22 < b* < -24) and a fair performance in glassy coatings, fired over 1000ºC (-12 < b* < -19). Nevertheless, it can be observed a limited colour development in low temperatures glassy coatings up to 1000 ºC, likely because of the uncomplete incorporation of cobalt in the glassy matrix (b* ~6).

In reality, the cyan nano-pigment acts as a dye, as neither crystalline $CoAl_2O_4$ nor other cobalt phases are detected inglazes. There is evidence that Co^{2+} is dissolved in the glasses in 4-fold coordination, which is typical in both silicate and borosilicate glasses [33] giving rise to the strong absorbance in the 14000-17000 cm^{-1} range. Although the occurrence of a small amount of Co^{2+} in octahedral coordination cannot be ruled out. Therefore, changes in colour after firing at low temperatures are likely linked to a varying ratio between tetrahedrally- and octahedrally-coordinated Co^{2+} and/or to a structural rearrangement of the Co^{2+} in the glass up to 1200 ºC.

The optical spectra of glassy coatings coloured with nano- and micro-$CoAl_2O_4$ are to a large extent superimposed (Fig. 3d), implying that also the micrometric pigment tends to be dissolved in ceramic matrices, since no peaks of cobalt aluminate spinel are detectable in the XRD patterns of glazes.

3.3. Yellow nano-pigment

The yellow nano-pigment is a Cr- and Sb-doped titania. Foreign-element-doping of titania is one of well-known methods to extend the absorption edge to the visible-light region by forming a donor or an acceptor level in the forbidden band [34]. Dopants such as Cr, Cd and Co ions, extend the spectral response of TiO_2 into the visible by inducing optical transitions from d electrons of the metal to the conduction band. In particular, chromium ions, substituting for Ti^{4+} in the TiO_2 lattice, have so far yielded optimal results [35]. The rutile structure is widely used as a host crystal in ceramic pigments, due to its capacity to develop an intense coloration when doped with transitions metals, along with a fair chemico-physical resistance at high temperature [36]. Chromium promotes a narrowing of the forbidden band, giving rise to orange hues, once a second element with high field strength (e.g. Sb) is added to achieve the electroneutrality of the structure, balancing the charge mismatch between Ti^{4+} and Cr^{3+} [37]. The X-ray diffraction, performed on glassy coatings coloured with the nano-pigment, reveals that the anatase structure is stable below 900 ºC; above this temperature, rutile is formed and withstand the chemical attack of the glassy phase at least to 1100 ºC. This implies a considerably increased thermal resistance of Cr-doped nanotitania, since undoped nano anatase usually transfroms into rutile around 500 °C [38] confirming previous data on the nano-ink [39]. No crystalline titania phases are found over 1200 ºC in glassy coatings. Rutile is not detectable in glazes, because of peak overlapping with opacifying phases (i.e. anorthite, zircon). The crystallite size of rutile increases regularly from 10 to 50 nm in the 800-1100 ºC range (Fig. 4) thus at a growth rate similar to that observed in nano rutile alone [40]. The UV-Vis spectra show an optical band at ~25000 cm^{-1} for the glassy coating F4, fired at 800 ºC, which shifts to ~22000 cm^{-1} in the case of glasses F1, F2 and F3 fired in the 900-1000 ºC range (Fig. 5a). A drastic change is observed in the glazes S1, S2 and S3, since there is no longer a single band, but distinct, weak peaks attributable to Cr^{3+} dissolved in the glassy matrix [32]. The

same evolution occurs in F1 fired at different temperatures (Fig. 5b): the optical band at the violet-UV border is connected with the occurrence of anatase at 800 °C; its shift to ~22000 cm^{-1} (900-1000 °C) is due to both the anatase-to-rutile transformation and particle growth, while the band disappearance at 1200 °C likely stands for TiO_2 dissolution in the ceramic matrix. Observing the colourimetric parameters (Table 2), it can be found that the deeper yellow colour component (b* ~40) is achieved with the Cr-doped anatase crystal structure (800 ºC) where the occurrence of Cr^{3+} is able just to shifts slighty the band energy. The anatase-to-rutile transition brings about an increased red component (a*~13) which is due to the changing band slope, provoking the absorption also of the blue light, so resulting in an orange shade promoted by crystallite size growth (Table 2). The colour deterioration at the highest temperature (b* ~20, a* <10) is consequent to decomposition of the crystalline TiO_2 phases. The occurrence of Cr^{3+} ions in the glass is able to explain this drastic colour change. At any rate, the pinkish colour of the glaze S3 could be related to a partial oxidation of Cr^{3+} to Cr^{4+} [41] which is rather frequent in ceramic pigments [42].

Ceramic wares coloured with titanium-based yellow pigments exhibit analogous optical spectra (Fig. 5c) with the main difference being the enhanced absorbance when micro-pigment is used. However, this different absorbance has important repercussions on coloration: the nano-pigment is characterized by a pure yellow shade, because its yellow component (b*) is higher and its red component (a*) is lower than those of the micro-pigment.

3.4. Black nano-pigment

The black nano-pigment was designed as a cobalt ferrite with spinel structure. The $CoFe_2O_4$ stoichiometry is expected to arrange in a partially inverse structure, with the Co^{2+} ion in both tetrahedral and octahedral sites [43-44]. Extensive Co-O and Fe-O charge transfers, together with d-d electron transitins of Co^{2+} and Fe^{3+} in multiple coordination, ensure the full absorption of the visible spectrum [20,31]

The $CoFe_2O_4$ structure is stable with temperature, besides crystallite size grows from 20 nm (800 ºC) to ~250 nm (1200 ºC). Such particle size growth is very fast in glassy coatings, but it seems to be prevented in glazes, where crystallite size persists in the 20-40 nm range (Fig. 6). The black colour, expressed as the lower colourimetric parameter L*, turns darker with temperature (Table 2) besides without regular trend, so an effect of particle size cannot be ruled out. The colour performance depends on the coating crystallization degree: the larger the amount of crystals formed in the glass, the brighter the colour (i.e. higher L* values). Considering only the glassy coating F1, it can be observed that the colour becomes more intense when firing temperature increases (Table 2). The other glassy coatings behave in the same way, but F4.

The comparison of black micro- and nano-pigments is difficult because the nano-ink, once applied in rather high amount, did not penetrate uniformly the unfired glaze layer, so the pigment distribution in the fired sample is not homogeneous and the uncoloured substrate appears in thin cracks. This can justify the clear difference of brightness between glazes coloured with micro- or nano-pigments. In any case, the chroma values (i.e. c* = |a*| + |b*|) are comparable in the glazes, even though some colour loss may occur in glassy coatings.

4. Conclusions

Ceramic nano-pigments, designed for quadrichromy (cyan, magenta, yellow and black) ink-jet printing of ceramic tiles, have been applied in several glazes and glassy coatings,

comparing their colour performance with that of correspondent conventional micro-pigments.

Each nano-pigment is characterized by its own colour mechanisms (i.e. surface plasmonic resonance for nanogold; Co^{2+} dissolution in the glassy phase for $CoAl_2O_4$; anatase-to-rutile transformation and change of the band structure induced by Cr^{3+}doping in nanotitania; extensive Co-O and Fe-O charge transfer in $CoFe_2O_4$).

The colour performance of ceramic pigments is a compromise between the efficiency of coloration, that is thought to be improved by small sizes, and dissolutions kinetics in the ceramic matrix, that is expected to be faster when particle size is reduced. From this standpoint, nano-pigments behave satisfactorily, bestowing intense colours on ceramic wares, besides their very small particle size (mostly <50 nm). However, the thermal stability depends on the type of nano-pigments and ceramic matrices, being high in the case of black, cyan and magenta colours, which are stable in the whole firing range tested (800-1200 ºC) although less intense colours are achieved with respect to conventional micro-pigments. Nanotitania is less stable at high temperature, but its yellow coloration is better than that of the correspondent micro-pigment.

Acknowledgements

CAPES (Coordenação de Aperfeiçoamento de Pessoal de Nível Superior, Brazil) is warmly acknowledged for supporting the post-doctorate fellowship (BEX 0151/07-6) of one of the authors (PMTC).

References

1] Cain M, Morrell R. Nanostructured ceramics: a review of their potential. Applied Organometallic Chemistry 2001;15:321-330.
2] Hu Z, Xue M, Zhang Q, Sheng Q, Liu Y. Nanocolorants: a novel class of colorants, the preparation and performance characterization. Dyes and Pigments 2008;76:173-178.
3] Maile FJ, Pfaff G, Reynders P. Effect pigments: past, present, and future. Progress in Organic Coatings 2005;54:150-163.
4] Sermone N, Dondi D, Albini A. Inorganic and organic UV filters: their role and efficacy in sunscreens and suncare products. Inorganica Chimica Acta 2007;360:794-802.
5] nGimat, nanoEngineered Materials, http://www.ngimat.com/nanotech/ cosmetics.html
6] Lim JH, Choi HK, Kwon JS, Lee KH, Kim SW, Kim MS, Chung CI, Lee JS. Development of high-contrast CRT based on nano pigment screen technique. Digest of Technical Papers - SID International Symposium 2005;36:1532-1535.
7] Wu H-T, Lee M-J, Lin H-M. Nano-particles formation for pigment red 177 via continuous supercritical anti-solvent process. Journal of Supercritical Fluids 2005;33:173-182.
8] Smith HM (ed.). High performance pigments. Weinheim: Wiley-VCH Verlag, 2002.
9] Perera DY. Effect of pigmentation on organic coating characteristics. Progress in Organic Coatings 2004;50:247-262.
10] Biswas SK, Dhak D, Pathak A, Pramanik P. Chemical synthesis of environment-friendly nanosized yellow titanate pigments. Materials Research Bulletin 2008;43:665-675.
11] Roqué J, Molera J, Sciau P, Pantos E, Vendrell-Saz M. Copper and silver nanocrystals in lustre lead glazes: development and optical properties. Journal of the European Ceramic Society 2006;26:3813-3824.
12] Roqué J, Pradell T, Molera J, Vendrell-Saz M. Evidence of nucleation and growth of metal Cu and Ag nanoparticles in lustre: AFM surface characterization. Journal of Non-Crystalline Solids 2005;351:568-575.
13] Borgia I, Brunetti B, Mariani I, Sgamellotti A, Cariati F, Fermo P, Mellini M, Viti V, Padeletti G. Heterogeneous distribution of metal nanocrystals in glazes of historical pottery. Applied Surface Science 2002;185:206-216.
14] Gardini D, Dondi M, Costa AL, Matteucci F, Blosi M, Galassi C, Baldi G, Cinotti E. Nano-sized ceramics inks for drop-on-demand ink-jet printing in quadrichromy. Journal of Nanoscience and Nanotechnology 2008;8:1978-1988.

15] Eppler RA. Colorants for ceramics. Kirk RE, Othmer DF, Encyclopedia of Chemical Technology, New York, Wiley 1998;6:877-892.
16] Baldi G, Bitossi M, Barzanti A. Patent WO 03/076521 A1, 2003.
17] Matteucci F, Lepri Neto C, Dondi M, Cruciani G, Baldi G, Boschi AO. Colour development of red perovskite pigment $Y(Al,Cr)O_3$ in various ceramic applications. Advances in Applied Ceramics 2006;105:99-106.
18] Tenório Cavalcante PM, Dondi M, Guarini G, Barros FM, da Luz AB. Ceramic application of mica titania pearlescent pigments. Dyes and Pigments 2007;74:1-8.
19] Patterson AL. The Scherrer formula for x-ray particle size determination. Physical Review 1939;56:978-982.
20] Marfunin S. Physics of minerals and inorganic materials. Berlin-Heidelberg-New York: Springer, 1979.
21] Berciaud S, Cognet L, Tamarat P, Lounis B. Observation of intrinsic size effects in the optical response of individual gold nanoparticles. Nano Letters 2005;5:515-518.
22] Sönnichsen C, Franzl T, Wilk T, Plessen G, Feldmann J. Drastic reduction of plasmon damping in gold nanorods. Physical Review Letters 2002;88:077402.
23] Vosburgh J, Doremus RH. Optical absorption spectra of gold nano-clusters in potassium borosilicate glass. Journal of Non-Crystalline Solids 2004;349:309-314.
24] Novo C, Gomez D, Juste-Perez J, Zhang Z, Petrova H, Reismann M, Mulvaney P, Hartland GV. Contributions from radiation damping and surface scattering to the linewidth of the longitudinal plasmon band of gold nanorods: a single particle study. Physical Chemistry Chemical Physics 2006;8:3540-3546.
25] Reillon V, Berthier S. Modelization of the optical and colourimetric properties of lustred ceramics. Applied Physics 2006;A83:257-265.
26] Lambies Lavilla V, Rincón Lopez JM. Study of the mechanism of formation of a zircon-cadmium sulphoselenide pigment. Transactions and Journal of the British Ceramic Society 1981;80:105-108.
27] Cruciani G, Matteucci F, Dondi M, Baldi G, Barzanti A. Structural variations of Cr-doped $(Y,REE)AlO_3$ perovskites. Zeitschrift für Kristallographie 2005;220:930-937.
28] Chen Z, Shi E, Li W, Zheng Y, Zhong W. Hydrothermal synthesis and optical property of nano-sized $CoAl_2O_4$ pigment. Materials Letters 2002;55:281-284.
29] Llusar M, Forés A, Badenes JA, Calbo J, Tena MA, Monrós G. Colour analysis of some cobalt-based blue pigments. Journal of European Ceramic Society 2001;21:1121-1130.
30] Monari G, Manfredini T. Coloring effects of synthetic inorganic cobalt pigments in fast-fired porcelainized tiles. Ceramic Engineering and Science Proceedings 1996;17(1):167-172.
31] Lever ABP. Inorganic electronic spectroscopy. 2nd ed. Amsterdam: Elsevier, 1984.
32] Keppler H. Crystal field spectra and geochemistry of transition metal ions in silicate melts and glasses. American Mineralogist 1992;77:62-75.
33] Keppler H, Bagdassarov N. The specification of Ni and Co in silicate melts from optical absorption spectra to 1500ºC. Chemical Geology 1999;158:105-115.
34] Umebayashi T, Yamaki T, Itoh H, Asai K. Analysis of electronic structures of 3d transition metal-doped TiO_2 based on band calculations. Journal of Physics and Chemistry of Solids 2002;63:1909-1920.
35] Borgarello E, Kiwi J, Grätzel M, Pelizzetti E, Viscald M. Visible light induced water cleavage in colloidal solutions of chromium-doped titanium dioxide particles. Journal of the American Chemical Society 1982;104:2996-3002.
36] Matteucci F, Cruciani G, Dondi M, Raimondo M. The role of counterions (Mo, Nb, Sb, W) in Cr-, Mn-, Ni- and V-doped rutile ceramic pigments. Part 1. Crystal strucuture and phase transformations. Ceramics International 2006;32:385-392.
37] Dondi M, Cruciani G, Guarini G, Matteucci F, Raimondo M. The role of counterions (Mo, Nb, Sb, W) in Cr-, Mn-, Ni- and V-doped rutile ceramic pigments. Part 2. Colour and technological properties. Ceramics International 2006;32:393-405.
38] Gilbert B, Zhang H, Huang F, Finnegan MP, Waychunas GA, Banfield JF. Special phase transformation and crystal growth pathways observed in nanoparticles. Geochemical Transactions 2003;4:20–27.
39] Matteucci F, Cruciani G, Dondi M, Baldi G, Dalconi MC, Barzanti A, Lorenzi G, Meneghini C. Structural modification of doped and undoped nanocrystalline TiO2 by temperature-resolved XRPD. Advances in Science and Technology 2006;51:99-104.
40] Nicula R, Stir M, Schick C, Burkel E. High-temperature high-pressure crystallization and sintering behavior of brookite-free nanostructured titanium dioxide: in situ experiments using synchrotron radiation. Thermochimica Acta 2003;403:129-136.
41] Pavlov RS, Marzá VB, Carda JB. Electronic absorption spectroscopy and colour of chromium-doped solids. Journal of Materials Chemistry 2002;12(9):2825-2832.

42] Doménech A, Torres FJ, Ruiz de Sola E, Alarcón J. Electrochemical Detection of High Oxidation States of Chromium (IV and V) in Chromium-Doped Cassiterite and Tin-Sphene Ceramic Pigmenting Systems. European Journal of Inorganic Chemistry 2006;638:638–648.
43] Ferreira TAS, Waerenborgh JC, Mendonça MHRM, Nunes MR, Costa FM. Structural and morphological characterization of $FeCo_2O_4$ and $CoFe_2O_4$ spinels prepared by a coprecipitation method. Solid State Sciences 2003;5:383-392.
44] Gabal MA, Ata-Allah SS. Effect of diamagnetic substitution on the structural, electrical and magnetic properties of $CoFe_2O_4$. Materials Chemistry and Physics 2004;85:104-112.

Table 1
Characteristics of ceramic nano-pigments and conventional ceramic micro-pigments used as reference.

	Pigment stoichiometry	Pigment concentration (wt. %)	Pigment particle size (90% within the range)
Nanopigments			
Cyan	$CoAl_2O_4$	2.6	10-20 nm
Magenta	Au^0	1.0	20-40 nm
Yellow	$(Ti,Cr,Sb)O_2$	6.0	10-20 nm
Black	$CoFe_2O_4$	18.7	20-30 nm
Micropigments			
Cyan	$CoAl_2O_4$	99	1-15 μm
Magenta	$Y(Al,Cr)O_3$	60	1-20 μm
	$Cd(S,Se):ZrSiO_4$	5	5-20 μm
Yellow	$(Ti,Cr,Sb)O_2$	70	5-30 μm
Black	$(Co,Fe)(Fe,Cr,Mn)_2O_4$	85	5-30 μm

Table 2
CIELab colourimetric parameters of nano-pigments dispersed in glassy coatings (F1, F2, F3 and F4) and glazes (S1, S2 and S3). Standard deviation of data is within 0.1.

Nano-pigment	Matrix	Firing temperature (ºC)	L*	a*	b*
Magenta Au^0	F1	800	46.2	26.0	3.5
	F1	900	40.4	31.6	6.9
	F1	1000	36.3	24.7	10.6
	F1	1100	36.9	24.0	9.0
	F1	1200	37.7	18.2	14.1
	F2	950	35.8	24.8	7.6
	F3	900	39.0	33.4	9.1
	F4	800	38.0	21.7	7.1
	S1	1200	48.4	15.6	6.3
	S2	1150	52.2	14.7	3.1
	S3	1100	56.1	15.6	-1.9
Cyan $CoAl_2O_4$	F1	800	50.7	-2.6	14.2
	F1	900	51.3	-1.5	-6.1
	F1	1000	48.8	1.1	-12.1
	F1	1100	39.5	4.7	-19.1
	F1	1200	34.3	1.6	-11.8
	F2	950	70.6	3.8	-4.0
	F3	900	48.9	-1.0	-6.9
	F4	800	42.5	5.8	-23.4
	S1	1200	40.4	5.3	-24.2
	S2	1150	42.8	4.9	-22.0
	S3	1100	58.0	3.5	-22.6
Yellow $(Ti,Cr,Sb)O_2$	F1	800	77.8	5.7	39.6
	F1	900	65.7	13.3	41.2
	F1	1000	65.9	11.8	40.6
	F1	1100	68.4	6.9	41.9
	F1	1200	59.9	1.7	20.8
	F2	950	62.6	13.9	38.7
	F3	900	65.6	14.6	41.5
	F4	800	74.1	1.3	39.7
	S1	1200	71.1	4.0	20.3
	S2	1150	69.7	8.4	20.5
	S3	1100	66.2	13.2	12.6
Black $CoFe_2O_4$	F1	800	34.9	2.0	1.5
	F1	900	40.3	0.8	1.3
	F1	1000	31.5	1.0	30.8
	F1	1100	28.6	0.8	0.8
	F1	1200	27.3	0.5	1.3
	F2	950	33.4	2.1	4.8
	F3	900	34.0	-0.1	-0.7
	F4	800	26.9	0.4	-2.3
	S1	1200	30.7	-0.3	-1.1
	S2	1150	30.2	-1.4	-2.7
	S3	1100	37.6	-2.5	-3.1

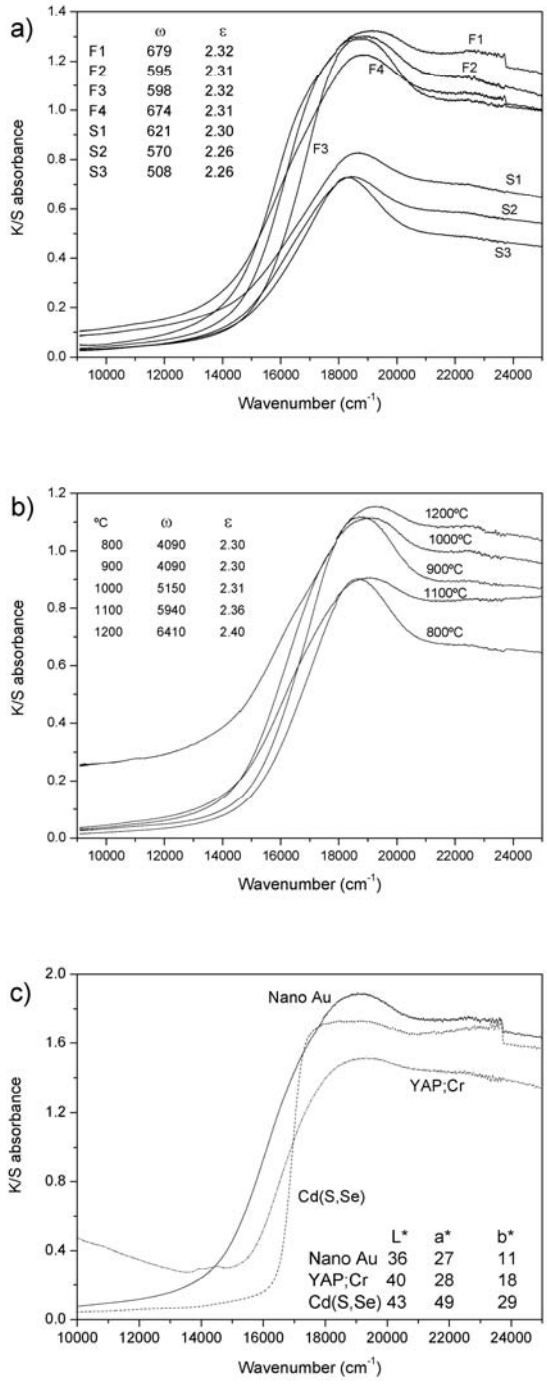

Fig. 1. Electron absorption spectra of gold nano-pigment: a) different glazes and glassy coatings; b) F1 fired at different temperatures; resonance energy of plasmonic band (ε, eV) and its FWHM (ω, meV) are reported in the insets. c) Comparison of the glassy coating F1 coloured with nanogold and commercial red micro-pigments (cadmium sulfoselenide and Cr-doped yttrium aluminium perovskite).

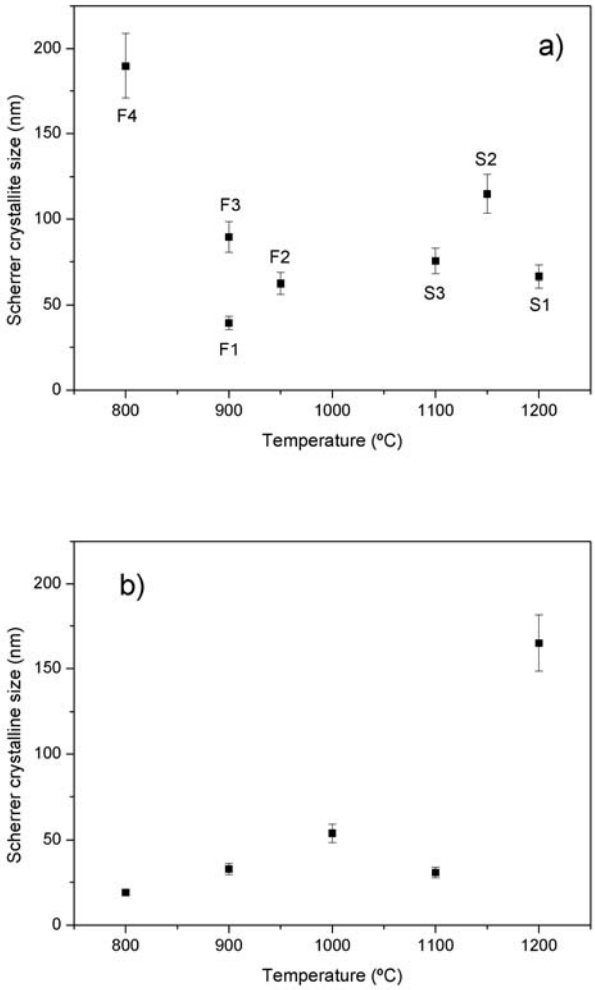

Fig. 2. Gold nano-pigment particle size in function of firing temperature: a) into different glazes and glassy coatings; b) into F1 glassy coating.

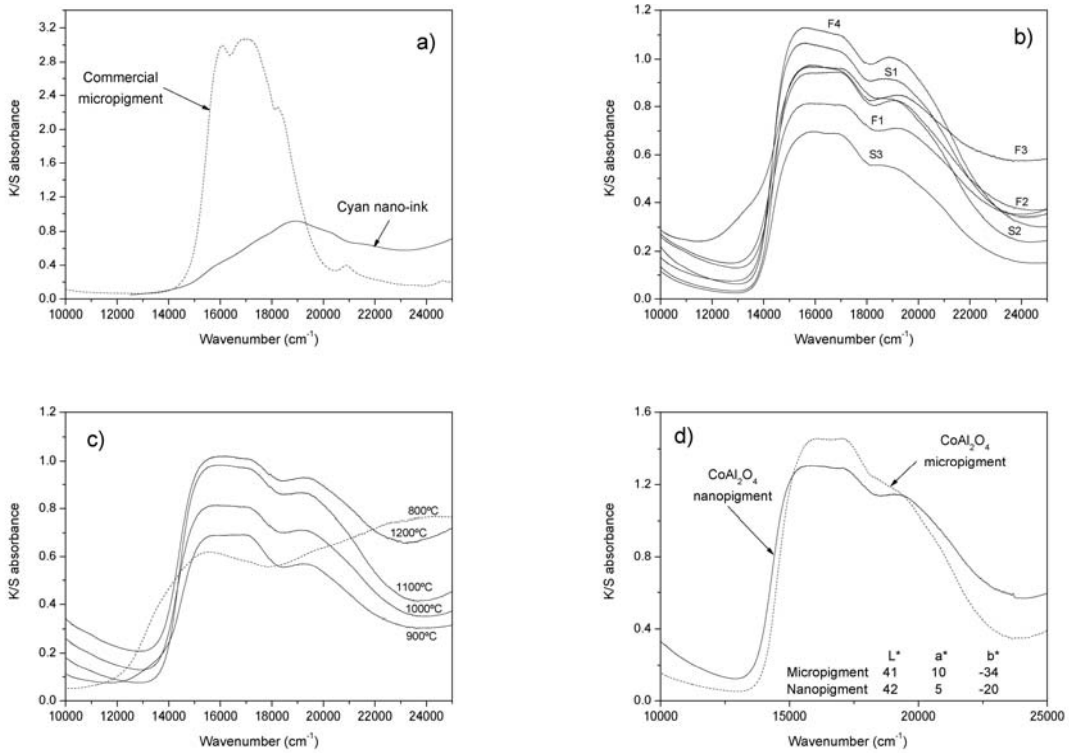

Fig 3. Electron absorption spectra: a) commercial micro-pigment and cyan nano-ink; b) different glazes and glassy coatings coloured with the cyan nano-pigment; c) glassy coating F1 coloured with the cyan nano-pigment and fired at different temperatures; d) comparison of the glassy coating F1 coloured with nano- and micro-pigment.

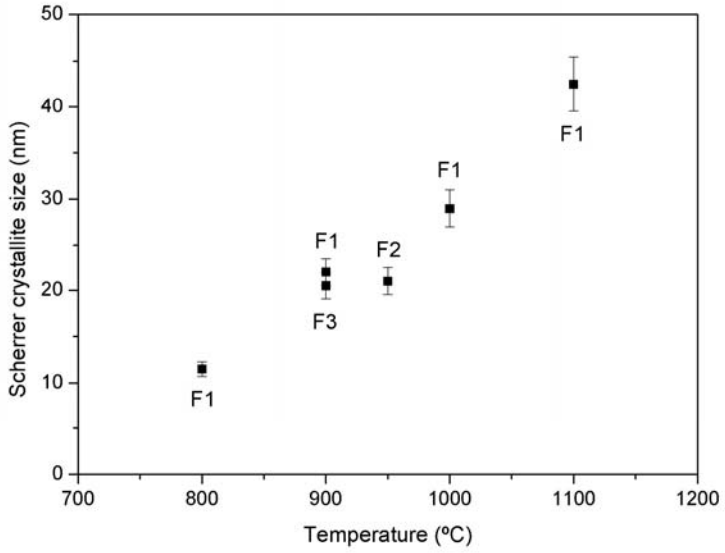

Fig. 4. Rutile particle size in function of firing temperature of the yellow nano-pigment into different glassy coatings.

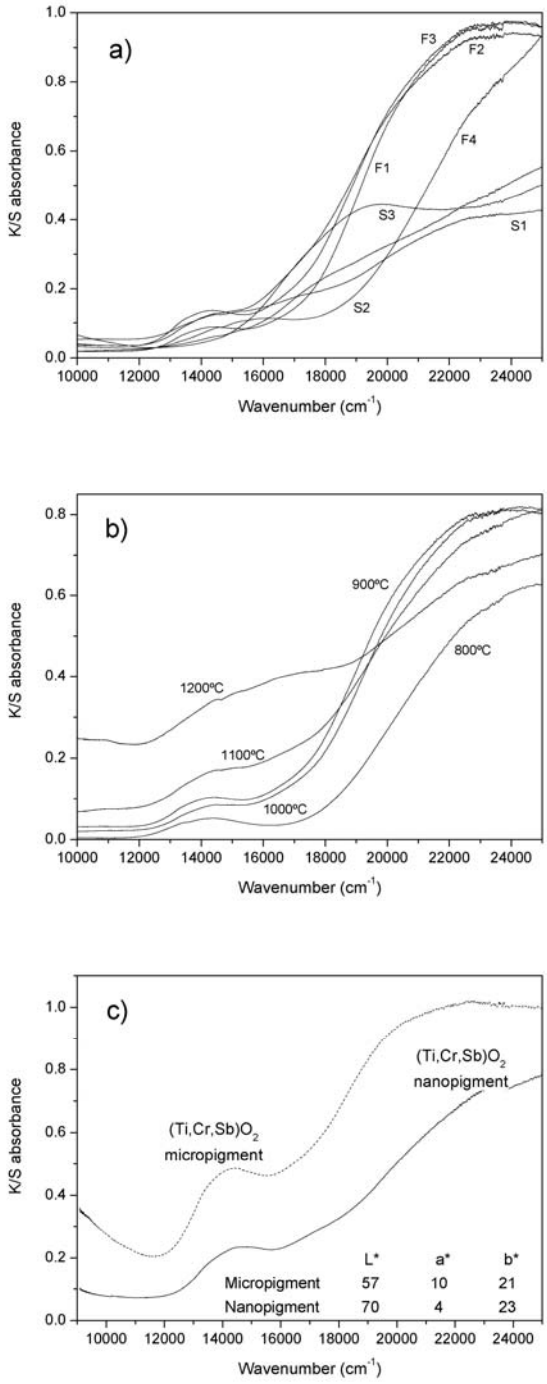

Fig. 5. Electron absorption spectra of ceramic wares coloured with yellow nano-pigment; a) different glazes and glassy coatings; b) glassy coating F1 fired at different temperatures; c) comparison of the glassy coating F1 coloured with nano- and micro-pigment.

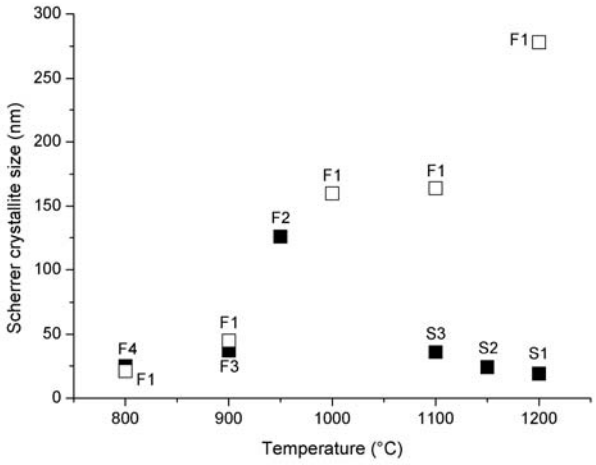

Fig. 6. The behaviour of the black nano-pigment particle size in function of firing temperature into different glazes and F1 glassy coating.